14

Tropical–extratropical interactions

Paul E. Roundy

14.1 INTRODUCTION

Intraseasonal anomalies of moist deep convection in the tropics evolve together with the global atmospheric circulation. Some of the coherence between tropical convection and extratropical weather is a consequence of redistribution of mass by convection, which is associated with broad-scale overturning circulations, global and regional cycles of atmospheric angular momentum (Anderson and Rosen, 1983; Weickmann and Sardeshmukh, 1994; Weickmann and Berry, 2009), and Rossby wavetrains that extend eastward and poleward across the midlatitudes (Sardeshmukh and Hoskins, 1988; Jin and Hoskins, 1995; Bladé and Hartmann, 1995). Another portion of this coherence is associated with modulation of tropical convection by extratropical waves (Lim and Chang, 1981; Webster and Holton, 1982; Hoskins and Yang, 2000; Allen *et al.*, 2008). Thus, the tropical and extratropical patterns influence each other, yielding profound associations between tropical intraseasonal oscillations and extratropical storm tracks. These associations frequently express themselves as global teleconnection patterns (Wallace and Gutzler, 1981; Ferranti *et al.*, 1990; Higgins and Mo, 1997, Matthews and Meredith, 2004; Cassou, 2008; L'Heureux and Higgins, 2008; Roundy and Verhagen, 2010). Prediction of midlatitude weather at lead times longer than 4 or 5 days thus depends on the geographical distribution and temporal evolution of moist deep convection in the tropics (Wallace and Gutzler, 1981; Ferranti *et al.*, 1990; Weickmann *et al.*, 1997; Mo and Higgins, 1998; Hendon *et al.*, 2000; Higgins *et al.*, 2000; Jones *et al.*, 2000; Nogues-Paegle *et al.*, 2000; Mo, 2000; Branstator, 2002; Jones *et al.*, 2004a,b; Weickmann and Berry, 2007). The global footprint of tropical intraseasonal oscillations allows them to influence or otherwise evolve with a broad range of high-impact weather events at high latitudes, including droughts and floods (Mo and Higgins, 1998; Jones, 2000; Higgins *et al.*, 2000; Whitaker and Weickmann, 2001; Jones *et al.*, 2004b; Donald *et al.*, 2006), extreme temperature events (Vecchi

W. K. M. Lau and D. E. Waliser (Editors), *Intraseasonal Variability in the Atmosphere–Ocean Climate System* (Second Edition).

and Bond, 2004; Lin and Brunet, 2009), and even the general timing and locations of outbreaks of severe thunderstorms and tornados.

Although convection in the tropics varies across a broad spectrum, the earliest analyses of connections between organized convection in the tropics and the flow throughout the global atmosphere were performed to study seasonal circulation patterns associated with El Niño and the Southern Oscillation (ENSO). More recently, interest has risen in the intraseasonal band. This band includes the Madden–Julian Oscillation (MJO), various convectively coupled equatorial waves, oceanic waves that might couple to atmospheric convection (e.g., Lau and Shen, 1988), and other disturbances. Some authors have demonstrated that equatorial Rossby waves and convectively coupled atmospheric and oceanic Kelvin waves are associated with variations in extratropical circulation (e.g., Matthews and Kiladis, 1995; Straub and Kiladis, 2003; Roundy, 2008; Roundy *et al*., 2010). However, much of the research that has associated tropical convection organized on intraseasonal timescales with the global flow has focused on the MJO, leading to a similar focus for this chapter.

Teleconnection patterns around the global extratropics have been analyzed for decades, but only since the early 1980s have the connections between these patterns and the MJO been manifest in the literature. Weickmann (1983) initiated analysis of observed connections between tropical convection organized on intraseasonal timescales and extratropical flow. He calculated the leading empirical orthogonal functions (EOFs) of pentad-averaged outgoing longwave radiation (OLR) anomalies in the tropics as well as the leading EOFs of pentad-averaged wind data from the upper and lower troposphere. He observed that during some northern hemisphere winters, eastward-moving convective anomalies in the tropics evolve together with anomalies in extratropical flow. Subsequently, Weickmann *et al*. (1985) applied cross-spectrum analysis between OLR anomalies and the 250 hPa streamfunction. Their results demonstrate, for example, that the circumpolar vortex expands southward along the longitudes of enhanced convection in the equatorial region and retracts northward along the longitudes of suppressed convection.

Following the initial work of Weickmann (1983) and Weickmann *et al*. (1985), Lau and Phillips (1986) showed coherent fluctuations between extratropical flow and eastward-moving anomalies of convection in the tropics of the eastern hemisphere. Observational and model analyses from the same decade and since have added further detail to the nature of observed associations between intraseasonal tropical convection and the flow throughout the global atmosphere (e.g., Knutson and Weickmann, 1987; Hsu *et al*., 1990; Hendon and Salby, 1994; Hsu, 1996; Matthews *et al*., 2004). Hsu (1996) argues—in agreement with Lau and Phillips (1986)—that the intraseasonal oscillation is a global phenomenon and that it is inadequate to treat it as either purely tropical or purely extratropical. Thus, the extratropical patterns associated with the oscillation in tropical convection might evolve as part of the fundamental anatomy of the oscillation itself, a possibility largely ignored in many of the simple models that have attempted to describe the MJO.

14.2 A BOREAL WINTER COMPOSITE OF THE GLOBAL FLOW ASSOCIATED WITH THE MJO

The seasonally varying global weather patterns associated with the MJO are easily diagnosed from observed and reanalysis data. The simplest demonstration of the general association of the MJO with the flow in the global atmosphere is a composite average of variables that characterize that flow, based on periods of time when the MJO evolved through particular phases. The Wheeler–Hendon (2004) real time multivariate MJO (RMM) indices offer a convenient basis for such composites, especially since these indices have been applied widely in recent years (for an overview, see Chapter 12).

Composites of the global flow associated with particular phases of the RMM indices during a particular season are easily calculated by averaging fields of data over the dates when the RMM indices suggest a given phase and when the MJO is active as suggested by the square root of the sum of the squares of the two indices exceeding 1 standard deviation (in practice, this occurs roughly 62% of the time in the 1974–2009 data, as shown by direct analysis of the two indices). We include here, for reference, such a composite for events during December through February. Figure 14.1 shows composite 300 hPa geopotential height (contours) together with OLR anomalies (shaded, with negative anomalies in blue, plotted only in the tropics, for simplicity). Panels (a)–(h) give the results for RMM phases 1–8, respectively. The pair of composites in each row represent nearly opposite phases of the oscillation. The regions shaded blue (suggestive of enhanced convection) tend to progress eastward with increasing phase number. The largest composite height anomalies exceed 100 m. Composite height anomaly fields do not always appear to evolve continuously from one RMM phase to the next. However, most of the associated patterns evolve continuously and smoothly between the phases when observed in daily means (not shown). Height anomalies move generally eastward through the tropics, with ridges amplifying over time poleward of the regions of enhanced convection and troughs amplifying poleward of the regions of suppressed convection. For example, during phases 1–5, convection begins and amplifies eastward across the Indian Ocean basin and the maritime continent. As this convection amplifies, a trough anomaly over southern Asia is gradually replaced by a ridge anomaly that later extends eastward across the Pacific following the convection. Similarly, during phases 5–8, a ridge that occurs north of a region of amplifying suppressed convection over the Indian Ocean basin (phase 5) decays during phase 6 and then a trough anomaly amplifies and extends eastward following the region of suppressed convection.

These ridge and trough anomalies across the subtropics associate with wavetrains that frequently extend away from the tropics even to near the poles. Many authors have thus demonstrated large signals associated with the MJO in the Arctic and Antarctic oscillations (Carvalho *et al.*, 2005; Zhou and Miller, 2005; L'Heureux and Higgins, 2008), the Pacific North America pattern (e.g., Mori and Watanabe, 2008), and the North Atlantic oscillation (e.g., Cassou, 2008; Roundy *et al.*, 2010). Figure 14.1 suggests that the highest amplitude anomalies of

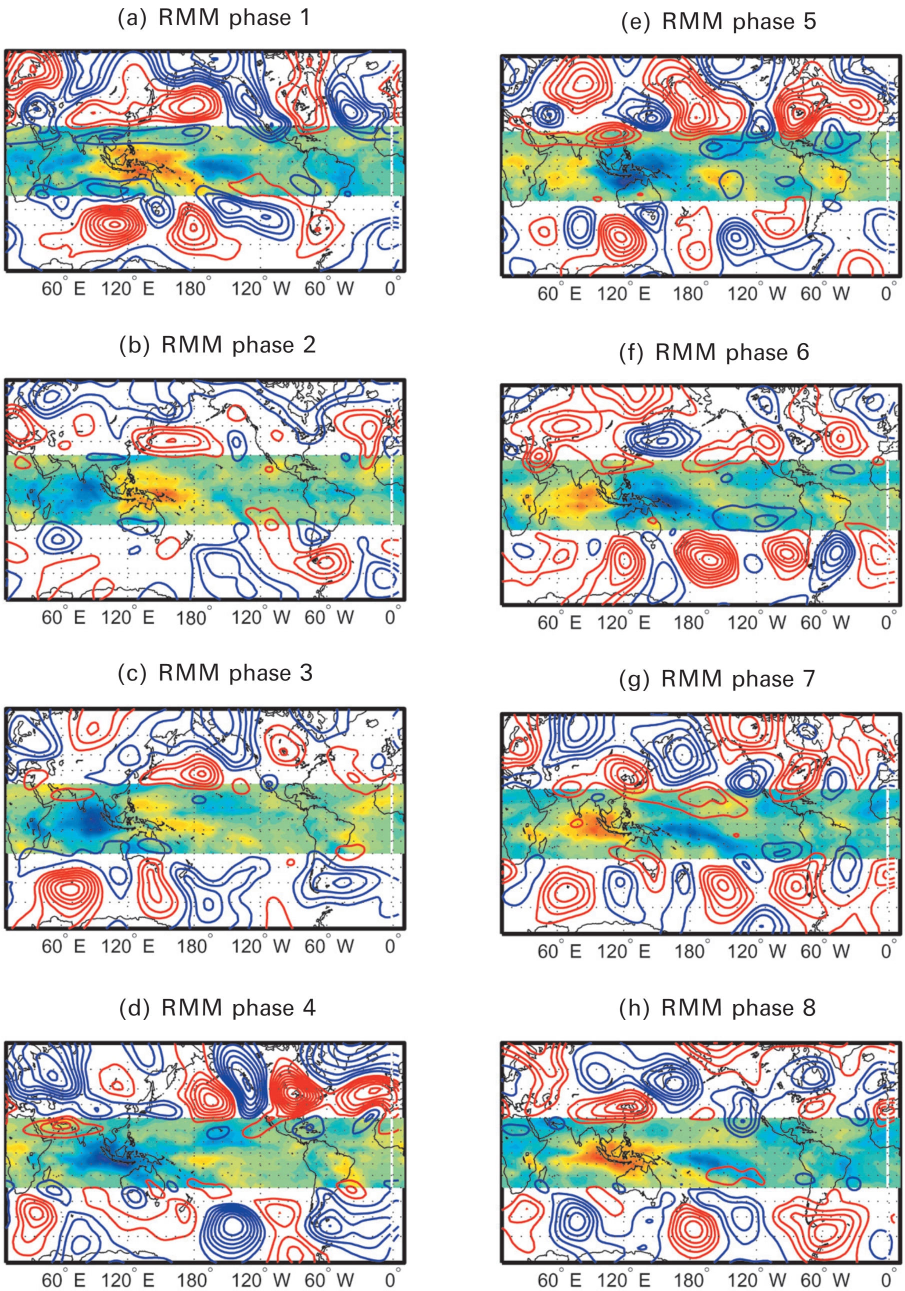

Figure 14.1. Composite OLR anomalies averaged over December through February (shaded, with negative anomalies suggestive of active convection in blue), and 300 hPa geopotential height anomalies (positive in red and negative in blue, with a contour interval of 15 m, and the zero anomaly is omitted). Panels (a)–(h) represent RMM phases 1–8, respectively.

300 hPa geopotential height associated with the MJO occur over the North Pacific and North Atlantic Oceans. The extratropical patterns associated with the MJO vary dramatically in both phase and amplitude with the status of ENSO and its temporal trend, as illustrated by the finding that composite signals in extratropical circulation associated with the MJO are substantially and significantly larger and found in different geographical locations when MJO events included in the averages are further sorted according to the ENSO phase in which they occur (Roundy *et al.* 2010).

Although the signals in OLR and geopotential height in Figure 14.1 are usually roughly opposite for the opposite panels within each row, some exceptions occur. These exceptions suggest asymmetries about the MJO cycle. However, some such asymmetries also result from a slightly different set of events averaged into the different phases. For example, some individual events might only attain the 1 standard deviation threshold during one or two phases, so the global pattern associated with those events would be included only in those phases. Such variation in RMM amplitude across the different phases during the same MJO event can sometimes be quasi-systematic. For example, the high-amplitude signals associated with one RMM phase at a given geographical location might occur during one ENSO state but not another. During development of La Niña conditions, high-amplitude expressions of RMM 6 and 7 are relatively infrequent, whereas phases 2–5 occur more often. Since the structure of the MJO and its associated global patterns change with ENSO (Roundy *et al.*, 2010), these changes would be expressed in Figure 14.1 as signals that are not opposite between opposite phases.

This composite analysis diagnoses the association between the MJO and extratropical signals, but it does not explain how these signals became associated with the MJO in the first place. Such associations could arise from a response of the global flow to heating in convection and/or from a response of convection to variations in extratropical flow. Most authors who have analyzed associations between flow in the extratropical atmosphere and the MJO have addressed this issue from one of these perspectives or the other rather than considering both directions of action simultaneously.

14.3 RESPONSE OF THE GLOBAL ATMOSPHERE TO HEATING IN TROPICAL CONVECTION

The global atmospheric circulation responds to heating in organized convection moving through the tropics (e.g., Bladé and Hartmann, 1995; Jin and Hoskins, 1995; Hendon and Salby, 1996; Matthews *et al.*, 2004). This response pattern includes overturning circulations through the tropics and Rossby wavetrains that extend poleward and around the globe. Jin and Hoskins (1995) force a simple model atmosphere in a DJF background state by a heat source fixed in space, with heating distributed in the vertical with a maximum heating rate near the 0.4 sigma level centered near the intersection of the equator and the dateline. Figure 14.2 shows the resulting equatorial cross-section of perturbation zonal flow after the heating

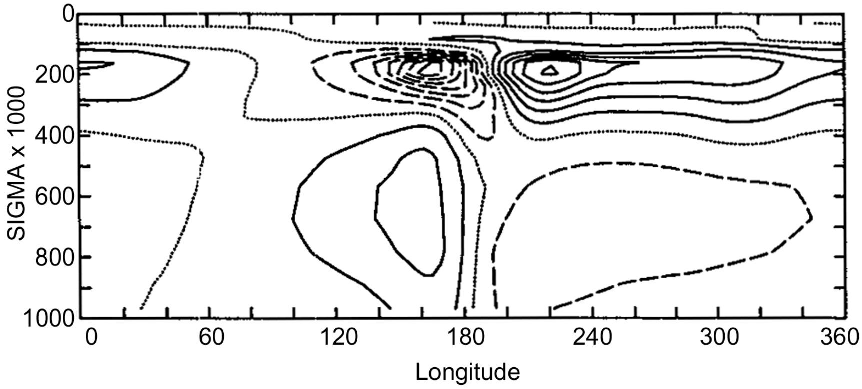

Figure 14.2. Vertical profile of a model response of zonal winds to heating on the equator (from Jin and Hoskins, 1995). This pattern develops after 15 days of heating, with a heating rate that increases with height from the surface of the earth to 0.4 sigma then decreases in intensity to zero near the tropopause. Heating is centered on the equator at the dateline. A background state equivalent to that of December through February is also assumed. Solid lines indicate westerly anomalies and dashed lines easterly anomalies.

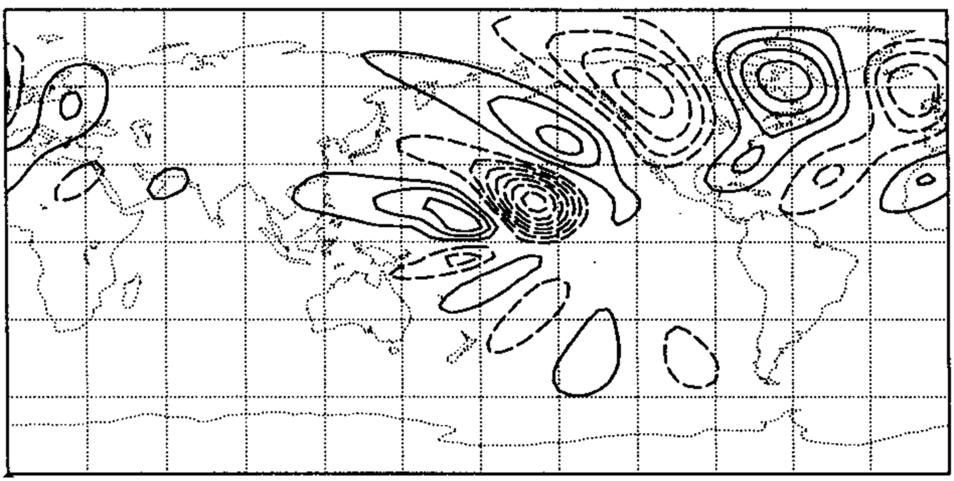

Figure 14.3. The horizontal pattern of streamfunction on the 0.24 sigma surface corresponding to the vertical cross-section shown in Figure 14.2. A northern hemisphere anticyclone is indicated by solid contours (from Jin and Hoskins, 1995).

continued for 15 days. Figure 14.2 demonstrates that the primary result of such heating in the equatorial plane is a vertical overturning circulation with an ascending branch in the vicinity of the heat source. Figure 14.3 shows the corresponding global pattern of streamfunction on the 0.24 sigma surface. This result indicates that upper-tropospheric ridges develop on the poleward sides of the heat source. These ridges are a consequence of mass redistributed as the atmosphere expands in response to the heating. As the upper-level flow accelerates poleward in response to associated pressure gradient forces, the Coriolis force and the beta effect induce anticyclinic upper-level flow (the beta effect may be larger because of the proximity to the equator). This geostrophic adjustment process also yields development of a trough downstream from the ridge. This pattern of downstream development is manifest as Rossby wave dispersion from the heat source toward the poles, deflected eastward by the prevailing westerly flow. The amplitude of the Rossby wave response is greatest across the winter hemisphere.

To diagnose the more specific response to patterns of convection more like those of the observed MJO, Matthews *et al.* (2004) force a primitive equation spectral transform model in a DJF background state with patterns of prescribed heating characteristic of the observed MJO. The flow in the model tropics characteristic of the MJO developed after a few days of initiating the prescribed heating and anomalies developed across the extratropics after about 2 weeks. The resulting global response to that heating is similar in many respects to the regression models and composite averages of observed data that show the actual weather patterns that associate with the MJO. However, the model result for the midlatitude circulation is shifted roughly 20 degrees of longitude from the observed pattern. Matthews *et al.* (2004) suggest that this phase shift might be associated with lack of a damping process in the regions of convective heating in their model.

14.4 INFLUENCE OF EXTRATROPICAL WAVES ON TROPICAL CONVECTION

Analysis of the influence of extratropical waves on tropical convection commenced before Weickmann (1983) diagnosed associations between tropical intraseasonal oscillations and the extratropical flow. Early works demonstrated that extratropical waves propagate into the tropics through regions of westerly wind (Lim and Chang, 1981; Webster and Holton, 1982), where they modulate tropical convection over a range of timescales that include those of the MJO (e.g., Matthews and Kiladis 1999a). Liebmann and Hartmann (1984) demonstrate large correlations between tropical convection and extratropical wave patterns and argue that most of the covariance in 5 and 10-day averaged data is associated with forcing of tropical convection by the extratropical flow, rather than the other way around. Hoskins and Yang (2000) further show that extratropical waves that merely propagate parallel to the tropics can also disturb the equatorial waveguide and help organize convection in the tropics, even if extatropical waves do not propagate directly into the tropics through regions of westerly wind. In an intermediate complexity model, Lin *et al.* (2000) show that extratropical wave activity could interact with wind–evaporation feedback in the tropics to generate patterns in the tropics that evolve like the MJO. More recently, Ray *et al.* (2009) and Ray and Zhang (2010) showed that a dry-channel model of the tropical atmosphere developed MJO-like signals in tropical wind fields when forced by reanalysis fields at poleward boundaries, but did not develop such signals internally when forced at the periphery by climatological winds. These results suggested to Ray *et al.* that extratropical patterns might force the organization of the MJO itself.

Extratropical waves also influence the organization of convection in the tropics on timescales shorter than those of the MJO. Such waves might influence progression of the MJO through some rectification process. For example, Rossby waves in the 6 to 30-day band propagate equatorward into the eastern equatorial Pacific basin, where they trigger convection along the ITCZ (Kiladis and Weickmann, 1992). Matthews and Kiladis (1999a) demonstrate that the convection that develops in the East Pacific ITCZ region in association with these extratropical waves rectifies back onto MJO timescales. This rectified signal in active convection moves eastward across the East Pacific to the east of the core of the MJO active convection, which occurs simultaneously over the West Pacific. In addition to the tropical convection organized by direct propagation of extratropical waves into the tropics through regions of westerly wind, further observational analyses show that convectively coupled Kelvin waves develop in association with extratropical waves, even in regions of easterly background flow that would prevent direct propagation into the tropics (Straub and Kiladis 2002), consistent with the model analysis of Hoskins and Yang (2000).

14.5 TWO-WAY INTERACTIONS BETWEEN THE TROPICS AND EXTRATROPICS

Some early authors acknowledged the possibility of two-way interactions between organized convection in the tropics and circulation in the extratropical atmosphere. Such interactions might facilitate the development of coherent circulation anomalies across the two regions (e.g., Lau and Phillips, 1986). The vast majority of more recent works, however, have emphasized either forcing of the tropics by extratropical waves or forcing of extratropical waves by tropical convection. Coherent circulation anomalies that bridge the tropics and the extratropics might be possible in part because the midlatitude response to tropical convection in one region can subsequently influence the evolution of convection elsewhere in the tropics. For example, a Rossby wavetrain forced by convection over Indonesia during the local active convective phase of the MJO acts to enhance convection farther east within the South Pacific Convergence Zone (Matthews and Meredith, 2004). Extratropical waves propagate into the tropics of the eastern equatorial Pacific as the MJO and ENSO combine to induce westerly winds across the region (Matthews and Kiladis, 1999a). Such extratropical wavetrains occasionally develop in association with the MJO and convectively coupled Kelvin wave activity farther west. In summary, these results suggest that:

(1) The MJO and other phenomena of organized tropical convection can induce extratropical waves.

(2) The circulation associated with the combination of the MJO and the background state can later guide the extratropical waves in (1) back into or parallel to the tropics in other geographical regions.
(3) These extratropical waves disturb the equatorial waveguide and further influence the local development and organization of convection associated with the MJO.
(4) The tropical convection influenced by extratropical waves can then redistribute mass, yielding Rossby wave dispersion to the extratropics, resulting in a continuously interactive feedback loop.

Consistent with this view, Moore *et al*. (2010) demonstrate that Rossby waves initially forced by convection within the MJO frequently break across the subtropics and in turn modulate further development of tropical convection. Figure 14.4 illustrates how the active convective phase of the MJO approaching the maritime continent region is associated with Rossby wave development near South East Asia and extension of a subtropical jet stream eastward across the Central Pacific basin (figure adapted from Moore *et al*., 2010). An anticyclonic wave-breaking event frequently develops across the Central Pacific basin at this stage of the MJO, which yields an upper-level trough in the deep tropics. Although this trough enhances convection on its eastern side, it suppresses convection on its western side, reinforcing the suppressed convective phase of the MJO over the west central Pacific basin.

The above works taken together suggest that the MJO might influence extratropical flow and then in turn be modulated thereby. Apparent dependence of the MJO on baroclinic instability along the subtropical jet stream (e.g., Straus

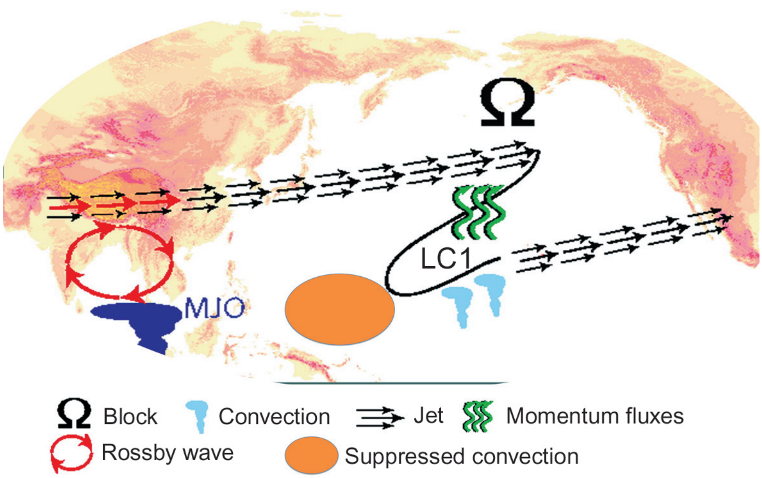

Figure 14.4. Schematic representation of the MJO and its associated patterns across higher latitudes as its active convection approaches the maritime continent, highlighting its association with breaking Rossby waves across the Central Pacific basin. LC1 refers to an anticyclonic wave-breaking event (adapted from Moore *et al*., 2010).

and Lindzen, 2000) suggests that these types of interactions between the MJO and the global flow might even be fundamental to the structure and evolution of the MJO itself (consistent with the model results of Lin *et al.*, 2000). In the context of the above results in which planetary waves respond to heating in convection within the MJO, the MJO-like wind signals in the tropical channel models of Ray *et al.* (2009) and Ray and Zhang (2010) might have developed at least in part because of extra-tropical signals in the reanalysis data that were forced by the MJO itself.

Accounting for such two-way interactions between the tropics and extratropics might help explain some discrepancies between model experiments and observations when authors assume that observed patterns might be forced exclusively by the tropics or exclusively by the midlatitudes. For example, part of the phase shift between the global response to MJO convection in the model of Matthews *et al.* (2004) and observed extratropical patterns might be associated with a lack of modulation of tropical convection by the extratropical flow in their model.

In spite of strong associations between tropical convection and higher latitude flow, both convection in the tropics and flow in the extratropical atmosphere contain substantial signals not explained by the other. Distinguishing the portion of the global flow anomaly that is associated with the MJO from the portion that is apparently not would benefit forecasters and other stakeholders. Some authors have developed algorithms for tracking the evolution of the MJO and extratropical patterns that frequently evolve with it. For example, Weickmann and Berry (2009) demonstrate that convection in the MJO frequently evolves together with a portion of the activity in a broader spectrum "global wind oscillation". They have developed indices for tracking the progress of this wind oscillation in near real time. The patterns commonly associated with the extratropical response to MJO convection are among the broader set of structures of this global wind oscillation.

14.6 MJO INFLUENCE ON THE PREDICTABILITY OF THE GLOBAL FLOW

The gradual evolution of tropical intraseasonal oscillations together with an understanding of the global circulation patterns that tend to evolve with them suggests that these oscillations might be applied to predict the evolution of a portion of the flow throughout the global atmosphere (Ferranti *et al.*, 1990). Traditional weather forecasting in the midlatitudes has developed one focus based largely on numerical weather prediction, which has generally been deemed most effective for forecast lead times shorter than roughly 1 week, and a second focus based on monthly (e.g., Vitart, 2004) or seasonal (e.g., Livezey and Timofeyeva, 2008; Preisendorfer and Mobley, 1984) prediction of the background climate state. Some forecasters have begun to apply understanding of tropical intraseasonal oscillations and their associations with midlatitude flows to help make predictions of midlatitude weather at lead times between the weekly and monthly forecast regimes.

Increased understanding of the observed teleconnection patterns associated with organized intraseasonal convection in the tropics has led to extension of skillful predictions of the evolving background state weather conditions around the globe into week 2 and beyond (e.g., Jiang *et al*., 2008; Vitart *et al*., 2008). By predicting the gradual evolution of the MJO (e.g., Waliser *et al*., 1999; Jiang *et al*., 2008; Gottschalk *et al*., 2010), it might be possible to use empirical means to predict the associated extratropical patterns. Such predictions straddle the weather–climate interface and have thus become of great interest in both private and government sectors.

Most empirical approaches to predict the extratropical patterns associated with tropical intraseasonal oscillations require first some choice of indices of the oscillations. Composite or linear regression analyses relate the selected indices to the corresponding "expectation values" of global weather patterns. Forecasts of future global patterns can be generated simply by introducing time lags into the composite or regression analyses or by predicting the indices themselves and referencing the corresponding favored global pattern for the target season (e.g., Jiang *et al*., 2008; Kang and Kim, 2010). Such predictions are more effective when global patterns are estimated based on events from similar ENSO states (e.g., Roundy *et al*., 2010).

Many of the statistical models applied for such prediction simply capitalize on observed patterns, regardless of the causes of those patterns. Such empirical prediction schemes are necessary because a consensus does not exist on the fundamental dynamics of the MJO itself and because most numerical models poorly simulate the MJO. Our apparent lack of understanding of the physics of the MJO thus does not prevent us from capitalizing on its signals to predict the evolutions of associated global flows. On the other hand, our lack of understanding of the dynamics of the MJO and our inability to simulate it properly is reflected in our lack of ability to predict the MJO beyond 30 days, or only about one half of an MJO cycle.

14.7 DISCUSSION

The MJO is associated with significant signals that extend around the globe and throughout the seasonal cycle. Organized convection in its active convective phase results in a planetary wave response that modulates teleconnection patterns around the globe. Convection organized in the tropics associated with the MJO is also strongly modulated by extratropical waves, including those that previously originated within the MJO itself. Such associations suggest the possibility that coupling between the tropics and the extratropics might be fundamental to the evolution and structure of the MJO. The associated global signals modulate extreme weather events. Since numerical weather prediction models tend to poorly simulate the MJO, MJO modulation of extreme events would reduce our ability to predict such events at long range by deterministic means until simulation of the MJO improves.

14.8 REFERENCES

Allen, G., G. Vaughan, D. Brunner, P. T. May, W. Heyes, P. Minnis, and J. K. Ayers (2008) Modulation of tropical convection by breaking Rossby waves. *Quart. J. Roy. Meteorol. Soc.*, **135**(638), 125–137, doi: 10.1002/qj.349.

Anderson, J. R. and R. D. Rosen (1983) The latitude–height structure of 40–50 day variations in atmospheric angular momentum. *J. Atmos. Sci.*, **40**, 1584–1591.

Arkin, P. and P. J. Webster (1985) Annual and interannual variability of tropical–extratropical interaction: An empirical study. *Mon. Wea. Rev.*, **113**, 1510–1523.

Bladé, I. and D. L. Hartmann (1995) The linear and nonlinear extratropical response to tropical intraseasonal heating. *J. Atmos. Sci.*, **52**, 4448–4471.

Brankovic, C., T. Palmer, and L. Ferranti (1994) Predictability of seasonal atmospheric variations. *J. Climate*, **7**, 217–237.

Branstator, G. W. (2002) Circumglobal teleconnections, the jet stream waveguide, and the North Atlantic Oscillation. *J. Climate*, **15**, 1893–1910.

Carvalho, L. M. V., C. Jones, and T. Ambrizzi (2005) Opposite phases of the Antarctic oscillation and relationships with intraseasonal to interannual activity in the tropics during austral summer. *J. Climate*, **18**, 702–718.

Cassou, C. (2008) Intraseasonal interaction between the Madden–Julian Oscillation and the North Atlantic Oscillation. *Nature*, **455**, 523–527.

Charney, J. and J. Shukla (1981) Predictability of monsoons. In: J. Lighthill and R. Pearce (Eds.), *Monsoon Dynamics*. Cambridge University Press, Cambridge, U.K., chap. 6.

Donald, A., H. Meinke, B. Power, M. C. Wheeler, A. de H.N. Maia , R. C. Stone, J. Ribbe, and N. White (2006) Near-global impact of the Madden–Julian Oscillation on rainfall. *Geophys. Res. Lett.*, **33**, L09704, 4 pp, doi: 10.1029/2005GL025155.

Ferranti, L., T. N. Palmer, F. Molteni, and K. Klinker (1990) Tropical–extratropical interaction associated with the 30–60 day oscillation and its impact on medium and extended range prediction. *J. Atmos. Sci.*, **47**, 2177–2199.

Frank, W. M. and P. E. Roundy (2006) The relationship between tropical waves and tropical cyclogenesis. *Mon. Wea. Rev.*, **134**, 2397–2417.

Frederiksen, J. S. and C. S. Frederiksen (1997) Mechanisms of the formation of intraseasonal oscillations and Australian monsoon disturbances: The roles of convection, barotropical and baroclinic instability. *Beitr. Phys. Atmos.*, **70**, 39–56.

Gottschalck, J., M. Wheeler, K. Weickmann, F. Vitart, N. Savage, H. Lin, H. Hendon, D. Waliser, K. Sperber, M. Nakagawa *et al.* (2010) A framework for assessing operational Madden–Julian Oscillation forecasts: A CLIVAR MJO Working Group project. *Bull. Amer. Meteorol. Society*, **91**, 1247–1258.

Gruber, A. (1974) The wavenumber–frequency spectra of satellite-measured brightness in the tropics. *J. Atmos. Sci.*, **31**, 1675–1680.

Hendon, H. H. and B. Liebmann (1991) The structure and annual variation of antisymmetric fluctuations of tropical convection and their association with Rossby–gravity waves. *J. Atmos. Sci.*, **48**, 2127–2140.

Hendon, H. H. and M. L. Salby (1994) The life cycle of the Madden–Julian Oscillation. *J. Atmos. Sci.*, **51**, 2225–2237.

Hendon, H. H. and M. L. Salby (1996) Planetary-scale circulations forced by intraseasonal variations of observed convection. *J. Atmos. Sci.*, **53**, 1751–1758.

Hendon, H. H., B. Liebmann, M. Newman, J. D. Glick, and J. E. Schemm (2000) Medium-range forecast errors associated with active episodes of the Madden–Julian oscillation. *Mon. Wea. Rev.*, **128**, 69–86.

Higgins, R. W. and K. C. Mo (1997) Persistent North Pacific circulation anomalies and the tropical intraseasonal oscillation. *J. Climate*, **10**, 223–244.

Higgins, R. W., J.-K. E. Schemm, W. Shi, and A. Leetmaa (2000) Extreme precipitation events in the western United States related to tropical forcing. *J. Climate*, **14**, 403–417.

Hoskins, B. J. and G.-Y. Yang (2000) The equatorial response to higher latitude forcing. *J. Atmos. Sci.*, **57**, 1197–1213.

Hsu, H.-H. (1996) Global view of the intraseasonal oscillation during northern winter. *J. Climate*, **9**, 2386–2406.

Hsu, H.-H., B. J. Hoskins, and F.-F. Jin (1990) The 1985/86 intraseasonal oscillation and the role of the extratropics. *J. Atmos. Sci.*, **47**, 823–839.

Jiang, X., D. E. Waliser, M. Wheeler, C. Jones, M.-I. Lee, and S. Schubert (2008) Assessing the skill of an all-season statistical forecast model for the Madden–Julian Oscillation. *Mon. Wea. Rev.*, **136**, 1940–1956.

Jin, F. and B. J. Hoskins (1995) The direct response to tropical heating in a baroclinic atmosphere. *J. Atmos. Sci.*, **52**, 307–319.

Jones, C. (2000) Occurrence of extreme precipitation events in California and relationships with the Madden–Julian Oscillation. *J. Climate*, **13**, 3576–3587.

Jones, C. and J.-K. E. Schemm (2000) The influence of intraseasonal variations on medium-range weather forecasts over South America. *Mon. Wea. Rev.*, **128**, 486–494.

Jones, C. (2000) Occurrence of extreme precipitation events in California and relationships with the Madden–Julian Oscillation. *J. Climate*, **13**, 3576–3587.

Jones, C., D. E. Waliser, K. M. Lau, and W. Stern (2004a) Global occurrences of extreme precipitation and the Madden–Julian Oscillation: Observations and predictability. *J. Climate*, **17**, 4575–4589.

Jones, C., D. E. Waliser, K. M. Lau, and W. Stern (2004b) The Madden–Julian oscillation and its impact on Northern Hemisphere weather predictability. *Mon. Wea. Rev.*, **132**, 1462–1471.

Kang, I.-S. and H.-M. Kim (2010) Assessment of MJO predictability for boreal winter with various statistical and dynamical models. *J. Climate*, **23**, 2368–2378.

Kiladis, G. N. and K. M. Weickmann (1992) Extratropical forcing of tropical Pacific convection during northern winter. *Mon. Wea. Rev.*, **120**, 1924–1938.

Kiladis, G. N. and M. C. Wheeler (1995) Horizontal and vertical structure of observed tropospheric equatorial Rossby waves. *J. Geophys. Res.*, **100**, 22981–22997.

Kiladis, G. N., C. D. Thorncroft, and N. M. J. Hall (2006) Three-dimensional structure and dynamics of African easterly waves, Part I: Observations. *J. Atmos. Sci.*, **63**, 2212–2230.

Kiladis, G. N., M. C. Wheeler, P. T. Haertel, K. H. Straub, and P. E. Roundy (2009) Convectively coupled equatorial waves. *Rev. Geophys.*, **47**, RG2003, doi: 10.1029/2008RG000266.

Knutson, T. R. and K. L. Weickmann (1987) 30–60 day atmospheric oscillations: Composite life cycles of convection and circulation anomalies. *Mon. Wea. Rev.*, **115**, 1407–1435.

Krishnamurti, T. N., P. K. Jayakumar, J. Sheng, N. Surgi, and A. Kumar (1985) Divergent circulations on the 30 to 50 day time scale. *J. Atmos. Sci.*, **42**, 364–375.

Lau, K.-M. and T. J. Phillips (1986) Coherent fluctuations of extratropical geopotential height and tropical convection in intraseasonal timescales. *J. Atmos. Sci.*, **43**, 1164–1181.

Lau, K.-M. and S. Shen (1988) On the dynamics of intraseasonal oscillations and ENSO. *J. Atmos. Sci.*, **25**, 1781–1797.

Liebmann, B. and D. L. Hartmann (1984) An observational study of tropical–midlatitude interaction on intraseasonal time scales during winter. *J. Atmos. Sci.*, **41**, 3333–3350

Liebmann, B. and H. H. Hendon (1990) Synoptic-scale disturbances near the equator. *J. Atmos. Sci.*, **47**, 1463–1479.

Liebmann, B. and C. A. Smith (1996) Description of a complete (interpolated) outgoing longwave radiation dataset. *Bull. Amer. Meteorol. Society*, **77**, 1275–1277.

Lim, H. and C. P. Chang (1981) A theory of midlatitude forcing of tropical motions during the winter monsoon. *J. Atmos. Sci.*, **41**, 3333–3350.

Lin, J.-L., G. N. Kiladis, B. E. Mapes, K. M. Weickmann, K. R. Sperber, W. Lin, M. C. Wheeler, S. D. Schubert, A. D. Genio, L. J. Donner *et al.* (2006) Tropical intraseasonal variability in 14 IPCC AR4 climate models, Part I: Convective signals. *J. Climate*, **19**, 2665–2690.

Lin, J. W.-B., J. D. Neelin, and N. Zeng (2000) Maintenance of tropical intraseasonal variability: Impact of evaporation–wind feedback and midlatitude storms. *J. Atmos. Sci.*, **57**, 2793–2823.

Lin, H., G. Brunet, and J. Derome (2009) An observed connection between the North Atlantic oscillation and the Madden–Julian oscillation. *J. Climate*, **22**, 364–380.

Lindzen, R. S. (1967) Planetary waves on beta planes. *Mon. Wea. Rev.*, **95**, 441–451.

Livezey, R. E. and M. M. Timofeyeva (2008) The first decade of long-lead U.S. seasonal forecasts: Insights from a skill analysis. *Bull. Amer. Meteorol. Society*, **89**, 843–854.

L'Heureux, M. L. and R. W. Higgins (2008) Boreal winter links between the Madden–Julian oscillation and the Arctic Oscillation. *J. Climate*, **21**, 3040–3050.

Madden, R. A. and P. R. Julian (1994) Observations of the 40–50-day tropical oscillation: A review. *Mon. Wea. Rev.*, **122**, 814–837.

Majda, A. J., B. Khouider, G. N. Kiladis, K. H. Straub, and M. G. Shefter (2004) A model for convectively coupled tropical waves: Nonlinearity, rotation, and comparison with observations. *J. Atmos. Sci.*, **61**, 2188–2205.

Matsuno, T. (1966) Quasi-geostrophic motions in the equatorial area. *J. Meteorol. Soc. Japan*, **44**, 25–43.

Matthews and Kiladis (1995) Please supply missing entry, see p. 494

Matthews, A. J. and G. N. Kiladis (1999a) The tropical–extratropical interaction between high-frequency transients and the Madden–Julian oscillation. *Mon. Wea. Rev.*, **127**, 661–677.

Matthews, A. J. and G. N. Kiladis (1999b) Interactions between ENSO, transient circulation, and tropical convection over the eastern tropical Pacific. *J. Climate*, **12**, 3062–3086.

Matthews, A. J. and G. N. Kiladis (2000) A model of Rossby waves linked to submonthly convection over the eastern tropical Pacific. *J. Atmos. Sci.*, **57**, 3785–3798.

Matthews, A. J. and M. P. Meredith (2004) Variability of Antarctic circumpolar transport and the Southern Annual Mode associated with the Madden–Julian Oscillation. *Geophys. Res. Lett.*, **31**, L24312, doi: 10.1029/2004GL021666.

Matthews, A. J., B. J. Hoskins, J. M. Slingo, and M. Blackburn (1996) Development of convection along the SPCZ within a Madden–Julian Oscillation. *Quart. J. Roy. Meteorol. Soc.*, **122**, 669–688.

Matthews, A. J., B. J. Hoskins, and M. Masutani (2004) The global response to tropical heating in the Madden–Julian oscillation during northern winter. *Quart. J. Roy. Meteorol. Soc.*, **130**, 1991–2011.

Mo, K. C. (2000) Intraseasonal modulation of summer precipitation over North America. *Mon. Wea. Rev.*, **128**, 1490–1505.

Mo, K. C. and R. W. Higgins (1998) Tropical influences on California precipitation. *J. Climate*, **11**, 412–430.

Molteni, F. and L. Ferranti (2000) *Non-linear Aspects of Systematic Errors of the ECMWF Coupled Model* (technical report). European Centre for Medium-Range Weather Forecasts, Reading, U.K.

Moore, R. W., O. Martius, and T. Spengler (2010) The modulation of the subtropical and extratropical atmosphere in the Pacific Basin in response to the Madden Julian Oscillation. *Mon. Wea. Rev.*, in press.

Mori, M. and M. Watanabe (2008) The growth and triggering mechanisms of the PNA: A MJO–PNA coherence. *J. Meteorol. Soc. Japan*, **86**, 213–236.

Nogues-Paegle, J., L. A. Byerle, and K. C. Mo (2000) Intraseasonal modulation of South American summer precipitation. *Mon. Wea. Rev.*, **128**, 837–850.

Pohl, B. and A. J. Matthews (2007) Observed changes in the lifetime and amplitude of the Madden–Julian oscillation associated with interannual ENSO sea surface temperature anomalies. *J. Climate*, **20**, 2659–2674.

Preisendorfer, R. W. and C. D. Mobley (1984) Climate forecast verifications: United States mainland, 1974–1983. *Mon. Wea. Rev.*, **112**, 809–825.

Ray, P. and C. Zhang (2010) A case study on the mechanisms of extratropical influence on the Madden–Julian Oscillation. *J. Atmos. Sci.*, **67**, 515-528.

Ray, P., C. Zhang, J. Dudhia, and S. S. Chen (2009) A numerical case study on the initiation of the Madden–Julian Oscillation. *J. Atmos. Sci.*, **66**, 310-331.

Roundy, P. E. (2008) Analysis of convectively coupled Kelvin waves in the Indian Ocean MJO. *J. Atmos. Sci.*, **65**, 1342–1359.

Roundy, P. E. and G. N. Kiladis (2006) Observed relationships between oceanic Kelvin waves and atmospheric forcing. *J. Climate*, **19**, 5253–5272.

Roundy, P. E. and J. R. Kravitz (2009) The association of the evolution of intraseasonal oscillations with ENSO phase. *J. Climate*, **22**, 381–395.

Roundy, P. E. and L. G. Verhagen (2010) Variations in the flow of the global atmosphere associated with a composite convectively coupled oceanic Kelvin wave. *J. Climate*, **23**, 4192–4201.

Roundy, P. E., K. MacRitchie, J. Asuma, and T. Melino (2010) Modulation of the global atmospheric circulation by combined activity in the Madden–Julian Oscillation and the El Niño/Southern Oscillation during boreal winter. *J. Climate*, **23**, 4045–4059.

Sardeshmukh, P. D. and B. J. Hoskins (1988) The generation of global rotational flow by steady idealized tropical divergence. *J. Atmos. Sci.*, **45**, 1228–1251.

Shinoda, T. and H. H. Hendon (2002) Rectified wind forcing and latent heat flux produced by the Madden–Julian Oscillation. *J. Climate*, **15**, 3500–3507.

Straub, K. H. and G. N. Kiladis (2002) Observations of a convectively coupled Kelvin wave in the eastern Pacific ITCZ. *J. Atmos. Sci.*, **59**, 30–53.

Straub, K. H. and G. N. Kiladis (2003) Interactions between the boreal summer intraseasonal oscillation and higher frequency tropical wave activity. *Mon. Wea. Rev.*, **131**, 945–960.

Straus, D. M. and R. S. Lindzen (2000) Planetary-scale baroclinic instability and the MJO. *J. Atmos. Sci.*, **57**, 3609–3626.

Vecchi, G. A. and N. A. Bond (2004) The Madden–Julian Oscillation (MJO) and northern high latitude wintertime surface air temperatures. *Geophys. Res. Lett.*, **31**, L24312, doi: 10.1029/2004GL021666.

Vitart, F. (2004): Monthly forecasting at ECMWF. *Mon. Wea. Rev.*, **132**, 2761–2779.

Vitart, F. *et al.* (2008) The new VAREPA-monthly forecasting system: A first step toward seemless prediction. *Quart. J. Roy. Meteorol. Soc.*, **134**, 1789–1799.

Waliser, D. E., K. M. Lau, and J.-H. Kim (1999) Influence of coupled sea surface temperatures on the Madden Julian Oscillation: A model perturbation experiment. *J. Atmos. Sci.*, **56**, 333–358.

Wallace, J. M. and D. S. Gutzler (1981) Teleconnections in the geopotential height field during Northern Hemisphere winter. *Mon. Wea. Rev.*, **109**, 784–812.

Webster, P. J. and J. R. Holton (1982) Cross-equatorial response to middle-latitude forcing in a zonally varying basic state. *J. Atmos. Sci.*, **39**, 722–733.

Weickmann, K. M. (1983) Intraseasonal circulation and outgoing longwave radiation modes during northern winter. *Mon. Wea. Rev.*, **111**, 1838–1858.

Weickmann, K. M. and E. Berry (2007) A synoptic–dynamic model of subseasonal atmospheric variability. *Mon. Wea. Rev.*, **135**, 449–474.

Weickmann, K. and E. Berry (2009) The tropical Madden–Julian oscillation and the global wind oscillation. *Mon. Wea. Rev.*, **137**, 1601–1614.

Weickmann, K. M. and P. D. Sardeshmukh (1994) The atmospheric angular momentum cycle associated with the Madden–Julian oscillation. *J. Atmos. Sci.*, **51**, 3194–3208.

Weickmann, K. M., G. R. Lussky, and J. E. Kutzbach (1985) A global scale analysis of intraseasonal fluctuations of outgoing longwave radiation and 250 mb streamfunction during northern winter. *Mon. Wea. Rev.*, **113**, 941–961.

Weickmann, K. M., G. N. Kiladis, and P. D. Sardeshmukh (1997) The dynamics of intraseasonal atmospheric angular momentum oscillations. *J. Atmos. Sci.*, **54**, 1445–1461.

Wheeler, M. and H. H. Hendon (2004) An all-season real-time multivariate MJO index: Development of an index for monitoring and prediction. *Mon. Wea. Rev.*, **123**, 1917–1932.

Wheeler, M. and G. N. Kiladis (1999) Convectively coupled equatorial waves: Analysis of clouds and temperature in the wavenumber–frequency domain. *J. Atmos. Sci.*, **56**, 374–399.

Wheeler, M. C. and K. M. Weickmann (2001) Real time monitoring and prediction of modes of coherent synoptic to intraseasonal tropical variability. *Mon. Wea. Rev.*, **129**, 2677–2694.

Whitaker, J. S. and K. M. Weickmann (2001) Subseasonal variations of tropical convection and week two prediction of wintertime western North American rainfall. *J. Climate*, **14**, 1524–1534.

Wilks, D. S. (2006) *Statistical Methods in the Atmospheric Sciences*. Academic Press, San Diego, CA, 627 pp.

Zhang, C. (2005) The Madden–Julian Oscillation. *Rev. Geophys.*, **43**, RG2003, doi: 10.1029/2004RG000158.

Zangvil, A. (1975) Temporal and spatial behavior of large-scale disturbances in tropical cloudiness deduced from satellite brightness data. *Mon. Wea. Rev.*, **103**, 904–920.

Zangvil, A. and M. Yanai (1981) Upper tropospheric waves in the tropics, Part II: Association with clouds in the wavenumber–frequency domain. *J. Atmos. Sci.*, **38**, 939–953.

Zhou, S. and A. J. Miller (2005) The interaction of the Madden–Julian Oscillation and the Arctic Oscillation. *J. Climate*, **18**, 143–159.